

Discovery of MK-3168: A PET Tracer for Imaging Brain Fatty Acid **Amide Hydrolase**

Ping Liu,**,† Terence G. Hamill, Marc Chioda,† Harry Chobanian,† Selena Fung,† Yan Guo,† Linda Chang,† Raman Bakshi,† Qingmei Hong,† James Dellureficio,† Linus S. Lin,† Catherine Abbadie,‡ Jessica Alexander,‡ Hong Jin,‡ Suzanne Mandala,‡ Lin-Lin Shiao,‡ Wenping Li,¶ Sandra Sanabria,¶ David Williams,¶ Zhizhen Zeng,¶ Richard Hajdu,§ Nina Jochnowitz,§ Mark Rosenbach,§ Bindhu Karanam, Maria Madeira, Gino Salituro,¶ Joyce Powell,¶ Ling Xu,¶ Jenna L. Terebetski,↓ Joseph F. Leone,† Patricia Miller,¶ Jacquelynn Cook,¶ Marie Holahan,¶ Aniket Joshi,¶ Stacey O'Malley,¶ Mona Purcell,¶ Diane Posavec,¶ Tsing-Bau Chen,¶ Kerry Riffel,¶ Mangay Williams,¶ Richard Hargreaves,¶ Kathleen A. Sullivan,‡ Ravi P. Nargund,† and Robert J. DeVita†

Supporting Information

ABSTRACT: We report herein the discovery of a fatty acid amide hydrolase (FAAH) positron emission tomography (PET) tracer. Starting from a pyrazole lead, medicinal chemistry efforts directed toward reducing lipophilicity led to the synthesis of a series of imidazole analogues. Compound 6 was chosen for further profiling due to its appropriate physical chemical properties and excellent FAAH inhibition potency across species. [11C]-6 (MK-3168) exhibited good brain uptake and FAAH-specific signal in rhesus monkeys and is a suitable PET tracer for imaging FAAH in the brain.

KEYWORDS: Fatty acid amide hydrolase, FAAH, positron emission tomography, carbon-11, PET tracer, target engagement, biomarker

atty acid amide hydrolase (FAAH) is a serine hydrolase characterized by an unusual Ser-Ser-Lys catalytic triad that cleaves amides and esters at similar rates. 1,2 It is an integral membrane enzyme responsible for the breakdown of several fatty acid ethanolamide (FAE) signaling molecules (Figure 1),

Figure 1. Substrates of fatty acid amide hydrolase.

including the endocannabinoid arachidonoyl ethanolamide (anandamide, AEA), and the related lipids N-palmitovl ethanolamide (PEA) and N-oleoyl ethanolamide (OEA).3-5 Inhibition of FAAH leads to elevated levels of these endogenous FAEs,6 which act on cannabinoid, vanilloid, and other receptors to induce anti-inflammatory, antidepressant, analgesic, and anxiolytic effects in preclinical animal models.⁷⁻⁹ In addition, these actions occur in the absence of the adverse

effects typically observed with direct cannabinoid receptor agonists. 10,11 Thus, FAAH represents a potential therapeutic target for the treatment of pain, inflammation, and other clinical disorders. Indeed, a number of FAAH inhibitors have been reported including covalent, irreversible inhibitors; covalent, reversible inhibitors; and noncovalent, reversible inhibitors. 12-16 To better understand FAAH biology and assist in the design and testing of promising drug candidates targeting this enzyme, a suitable FAAH positron emission tomography (PET) or single photon emission computed tomography (SPECT) radioligand is highly desirable, which would allow FAAH imaging studies in the living human and animal brain under normal physiological and diseased conditions. In general, a successful PET ligand should provide a good specific signal (total/nonspecific ≥ 1.5:1) to allow quantitative mapping of the target of interest. Though not an absolute, ideally, a brain PET ligand should have a good binding affinity with $B_{\text{max}}/K_{\text{d}} \ge$ 10 and reasonable lipophilicity with $\log P$ or $\log D$ of 1–3.5 for adequate brain penetration and optimum specific to nonspecific ratio. 17,18 Much effort has been devoted to the search for suitable FAAH PET ligands. The majority of the reported

Received: March 11, 2013 Accepted: April 20, 2013 Published: April 20, 2013

[†]Departments of Medicinal Chemistry, [‡]Immunology, [§]Pharmacology, [∥]Preclinical DMPK, [⊥]Basic Pharmaceutical Sciences, and *Process Research, Merck Research Laboratories, Rahway, New Jersey 07065, United States

[¶]Department of Imaging Research, Merck Research Laboratories, West Point, Pennsylvania 19486, United States

radioligands are URB597 analogues^{19,20} or anandamide analogues^{21,22} (Figure 2). Recent reports have appeared for

Figure 2. Representative examples of FAAH PET tracers.

[18F]PF-9811²³ and [11C-carbonyl]O-arylcarbamates²⁴ and the characterization of these tracers in rodents. Herein, we wish to report the discovery of a structurally distinct and reversible FAAH PET tracer (MK-3168) that may be suitable for clinical application.

The medicinal chemistry effort began with compound 2,²⁵ a potent FAAH inhibitor that had been identified from our lead optimization program. Compound 2 has an HPLC log *D* value of 4.2 and subnanomolar FAAH inhibition potency across species. Although the lipophilicity of compound 2 is higher than desired, we were encouraged by its excellent potency and decided to radiolabel compound 2. ¹¹CH₃ was introduced through precursor 1 to yield [¹¹C]-2 (Scheme 1). However, in

Scheme 1. Initial Efforts for a FAAH PET Tracer

vivo PET studies of [¹¹C]-2 in rhesus monkeys were complicated by brain-penetrant and radiolabeled metabolites, suggesting the need for a different scaffold for radiolabeling.

Our attention shifted to compound 3, another analogue from the pyrazole series²⁵ (Scheme 2). This compound has a reasonable FAAH inhibition potency in human and rat, but because rhesus monkey is our preferred preclinical species for evaluation of CNS PET tracers, its rhesus potency and lipophilicity required further optimization. More importantly, a reliable route to introduce a radiolabel to the molecule was needed since this was unable to be realized on compound 3. Thus, our structure—activity relationship (SAR) objective was to modify structure 3 to decrease lipophilicity, improve potency, and locate a structural feature for efficient radiolabeling.

Replacing pyrazole with imidazole is an effective way to lower $\log D$, provided other properties are maintained. In this regard, compound 4 (R = cyclopropyl) was synthesized; however, it was a much less potent compound (Scheme 2 and its table). To our delight, when R was changed to methyl (compound 5), the potency was improved by 3-fold; when R was removed (R = H; compound 6), the potency was improved significantly. However, compound 7, the imidazole regio isomer, and compound 8, the uncapped imidazole analogue, reduced potency by about 100-fold. With the $\log D$ of compound 6 in an acceptable range, the methyl substituent on the imidazole could serve as a handle to introduce 11 C. To further lower the $\log D$, primary amide 9 and secondary amide 10 were synthesized. While compound 9 was less potent than

Scheme 2. SAR Efforts and Identification of Compound 6

Cmpd	human ^a	rhesus ^{b,c}	rat ^a	HPLC Log D ^b
	IC_{50} (nM)	IC_{50} (nM)	IC_{50} (nM)	(pH 7.3)
3	5.0 ± 0.9	33	4.2 ± 0.3	3.8
4	48 ± 4.3	nd	106 ± 1.8	nd
5	13.6 ± 1.1	nd	34 ± 2.2	nd
6	1.0 ± 0.6	5.5 ± 3.8^{a}	1.7 ± 0.5	3.3
7	839 ± 145	nd	1388 ± 161	nd
8	650 ± 86	nd	145 ± 13	nd
9	3.3 ± 0.5	nd	12 ± 1.0	2.0
10	1.1 ± 0.3	nd	6.0 ± 1.6	2.9
11	3.2 ± 0.8	nd	4.8 ± 0.3	nd
12	1.5 ± 0.6	7.0	4.2 ± 0.3	3.0
13	3.0 ± 1.1	27	3.0 ± 0.7	3.4
14	0.3 ± 0.1	1.4	0.6 ± 0.2	4.2
15	0.8 ± 0.2	nd	1.7 ± 0.1	3.6
16	0.5 ± 0.1	nd	1.4 ± 0.0	3.8
17	1.0 ± 0.3	3.1	1.4 ± 0.1	4.0
18	1.1 ± 0.4	8.8	1.3 ± 0.4	4.3

^aFAAH inhibition IC₅₀ data expressed as mean \pm SD ($n \geq 2$ independent experiments). ^bnd = not determined. ^cAssayed only once except for compound **6**.

compound 6, compound 10 offered comparable potency. Furthermore, to consider the option of introducing ¹⁸F to the molecule, fluoroethyl analogues 11–13 were synthesized. Compounds 11 and 12 could be candidates for a ¹⁸F PET tracer, but analogue 13 was not an option due to its poor potency in rhesus, which is our preferred preclinical species for imaging studies. Finally, to complete the SAR studies, the chlorophenyl analogues 14–18 were also synthesized. These chlorophenyl analogues offered better potency (for example, 14 vs 6) but increased lipophilicity.

Compound **6** was chosen for further profiling. In the whole blood FAAH inhibition assay, compound **6** exhibited excellent potency in human (IC₉₀ = 5.5 nM) and rhesus (IC₉₀ = 29 nM). An off-target screen of this compound was performed against a panel of 168 receptors, ion channels, and enzymes; only two off-target activities, acetyl cholinesterase (IC₅₀ = 1.63 μ M) and phosphodiesterase PDE4 (IC₅₀ = 9.75 μ M), were identified. Compound **6** was very selective over the two key ion channels, hERG (IC₅₀ = 37 μ M) and DLZ (IC₅₀ = 16 μ M); CYP 3A4 (IC₅₀ > 50 μ M); as well as the two cannabinoid receptors, CB1 (IC₅₀ = 30 μ M) and CB2 (IC₅₀ = 150 μ M). This compound was not a substrate for rat or human P-glycoprotein in vitro and rapidly penetrated into the brain and achieved a brain-to-

plasma concentration ratio of 7:1 at 2 h following a 2 mg/kg oral dose to rats. On the basis of its overall profile, we believed compound **6** would provide a high probability of success to develop as a ¹¹C PET tracer.

The synthesis of [³H]-6 and [¹¹C]-6 is outlined in Scheme 3 and began with a Negishi-type coupling²⁷ between chiral

Scheme 3. Synthesis of $[^3H]$ -6 and $[^{11}C]$ -6

"Reagents and conditions: (a) **19**, EtMgBr, ZnCl₂ in THF, then **20** and Pd(PPh₃)₄, reflux, 72%; (b) 1 N HCl, MeOH, reflux, 66%; (c) NIS, dichloromethane, rt, 53%; (d) CuI, 1,10-phenanthroline, DMSO, 100 °C, 26%; (e) KOH, MeCN/water, 80 °C; (f) dimethylamine, HOBT, EDC, diisopropylethylamine, DMF, 72% for 2 steps; (g) CT₃I, Cs₂CO₃, DMF, rt; (h) [¹¹C]-MeI, Cs₂CO₃, DMF, 65 °C.

bromide 20²⁸ and the zinc species derived from the commercially available 19. This C–C bond formation provided compound 21 in 72% yield. After the trityl group was removed with HCl, imidazole 22 was converted by NIS to iodoimidazole 23 that was ready for the C–S bond formation. This C–S coupling proved challenging, most likely due to the interference of the free imidazole N–H.²⁹ In the end, the CuI-mediated coupling conditions were used for the reaction between iodoimidazole 23 and thiol 24²⁸ that afforded sulfide 25 in 26% yield. With intermediate 25 in hand, the remaining synthesis was straightforward. Ester hydrolysis and amide formation gave 8, a precursor to both [³H]-6 and [¹¹C]-6. Reaction of 8 with CT₃I provided [³H]-6. Finally, 8 was reacted with [¹¹C]-CH₃I completing the synthesis of PET tracer [¹¹C]-6.³⁰

[³H]-6 was used in tissue homogenate binding studies. As shown in Table 1, compound 6 exhibited excellent binding affinity to the cortex of rat, rhesus, and human. In addition,

Table 1. Tissue homogenate binding studies^a with [³H]-6

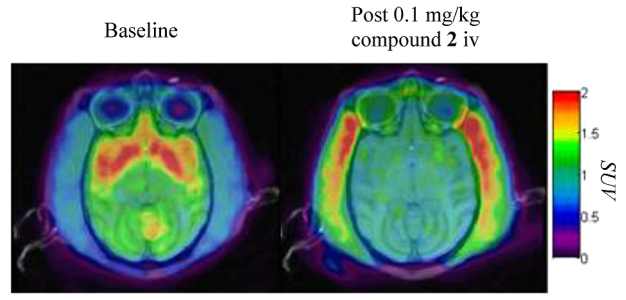
tissue	$K_{\rm d}$ (nM)	B_{max} (nM)	$B_{\rm max}/K_{\rm d}$
rat cortex	0.6 ± 0.1	43 ± 4	73 ± 11
rhesus cortex	1.4 ± 0.2	21 ± 3	15 ± 1
human cortex	0.8 ± 0.2	15 ± 1	19 ± 6

^aData expressed as mean \pm SD (n = 3 independent experiments).

Scatchard plot of transformed data showed that $[^3H]$ -6 bound to a single, saturable site in these species. 31 More importantly, the comparable $B_{\rm max}/K_{\rm d}$ ratio for rhesus monkey and human suggested that the magnitude of an observed in vivo specific signal of $[^{11}C]$ -6 in rhesus monkey could be similar to that in human.

The pharmaceutical properties of compound **6** were also assessed and the crystalline free base was characterized as its solid state form. This form of compound **6** showed excellent 24 h pH dependent solution stability, and solubility values obtained in 10 mM saline buffer at pH 3–8, with 10% ethanol, should provide adequate solubility to support clinical iv dosing.

[11C]-6 was evaluated in isoflurane-anesthetized rhesus monkeys as a potential PET ligand. Baseline scans after a single iv (5 mCi) administration revealed that [11C]-6 rapidly penetrated the blood/brain barrier and accumulated in the frontal cortex, striatum, and hippocampus regions (FAAH enriched area), 32 reaching a maximum signal in ~45 min. A blockade experiment was also carried out with compound 2, a potent FAAH inhibitor in rhesus (Figure 3). The total to



Summed images 60-90 min post tracer injection normalized to white-matter uptake, SUV.

Figure 3. In vivo PET images of [11 C]-6 in rhesus monkey brain. Color scale indicates standard uptake value (SUV) units (nCi/cc/mCi/kg).

nonspecific signal ratio was \sim 2:1, exceeding the targeted criteria 1.5:1. Table 2 compares the profile of [11 C]-6 against our target

Table 2. Comparison of Target Criteria and Profile of $[^{11}\mathrm{C}]\text{-}6$

target criteria for a FAAH PET tracer	[11C]- 6 profile
human $B_{\text{max}}/K_{\text{d}} > 10$	19
human $K_d < 2$ nM	0.8
moderate log D (1–3.5)	3.3
non- or weak substrate for hPGP (MDR)	0.8
$Papp > 20 \times 10^{-6} \text{ cm/s}^a$	$27 \times 10^{-6} \text{ cm/s}$
reliable route for C-11 or F-18 labeling	[¹¹ C]-MeI
good brain uptake in monkey	>1 SUV ^b
specific signal $\geq 1.5:1$ (total/nonspecific)	~2:1

"Measurement of cell permeability. "SUV: nCi/cc/mCi/kg body weight.

criteria for a FAAH PET tracer. We believe [11C]-6 has the criteria of a successful FAAH PET tracer and should find wide use for in vivo FAAH PET studies.

In summary, a high quality FAAH PET tracer [\$^{11}\$C]-6 (MK-3168) was developed through optimization of lipophilicity and potency for FAAH inhibition of the initial lead compound. This PET tracer exhibited good brain uptake and FAAH-specific signal in rhesus monkey PET studies and therefore was a suitable PET tracer for imaging FAAH in the brain. These results led to the decision to investigate [\$^{11}\$C]-6 in the clinic, which will be the subject of another publication.

ASSOCIATED CONTENT

S Supporting Information

Synthetic procedures and characterization data of selected compounds, conditions for the biological assays, reversibility study of compound **6**, and protocol for rhesus PET imaging. This material is available free of charge via the Internet at http://pubs.acs.org.

AUTHOR INFORMATION

Corresponding Author

*(P.L.) Phone: 732-594-0321. Fax: 732-594-9556. E-mail: ping liu2@merck.com.

Notes

The authors declare no competing financial interest.

ACKNOWLEDGMENTS

We thank the department of Laboratory Animal Resources for their assistance in animal dosing and sampling.

REFERENCES

- (1) Ahn, K.; McKinney, M. K.; Cravatt, B. F. Enzymatic pathways that regulate endocannabinoid signaling in the nervous system. *Chem. Rev.* 2008, 108, 1687–1707.
- (2) McKinney, M. K.; Cravatt, B. F. Structure and function of fatty acid amide hydrolase. *Annu. Rev. Biochem.* **2005**, *74*, 411–432.
- (3) Lambert, D. M.; Vandevoorde, S.; Jonsson, K. O.; Fowler, C. J. The palmitoylethanolamide family: A new class of anti-inflammatory agents? *Curr. Med. Chem.* **2002**, *9*, 663–674.
- (4) Devane, W. A.; Hanus, L.; Breuer, A.; Pertwee, R. G.; Stevenson, L. A.; Griffin, G.; Gibson, D.; Mandelbaum, A.; Etinger, A.; Mechoulam, R. Isolation and structure of a brain constituent that binds to the cannabinoid receptor. *Science* **1992**, *258*, 1946–1949.
- (5) Rodriguez de Fonseca, F.; Navarro, M.; Gomez, R.; Escuredo, L.; Nava, F.; Fu, J.; Murillo-Rodriguez, E.; Giuffrida, A.; LoVerme, J.; Gaetani, S.; Kathuria, S.; Gall, C.; Piomelli, D. An anorexic lipid mediator regulated by feeding. *Nature* **2001**, *414*, 209–212.
- (6) Cravatt, B. F.; Demarest, K.; Patricelli, M. P.; Bracey, M. H.; Giang, D. K.; Martin, B. R.; Lichtman, A. H. Supersensitivity to anandamide and enhanced endogenous cannabinoid signaling in mice lacking fatty acid amide hydrolase. *Proc. Natl. Acad. Sci. U.S.A.* **2001**, *98*, 9371–9376.
- (7) Lichtman, A. H.; Shelton, C. C.; Advani, T.; Cravatt, B. F. Mice lacking fatty acid amide hydrolase exhibit a cannabinoid receptormediated phenotypic hypoalgesia. *Pain* **2004**, *109*, 319–327.
- (8) Gaetani, S.; Dipasquale, P.; Romano, A.; Righetti, L.; Cassano, T.; Piomelli, D.; Cuomo, V. The endocannabinoid system as a target for novel anxiolytic and antidepressant drugs. *Int. Rev. Neurobiol.* **2009**, *85*, 57–72.
- (9) Gobbi, G.; Bambico, F. R.; Mangieri, R.; Bortolato, M.; Campolongo, P.; Solinas, M.; Cassano, T.; Morgese, M. G.; Debonnel, G.; Duranti, A.; Tontini, A.; Tarzia, G.; Mor, M.; Trezza, V.; Goldberg, S. R.; Cuomo, V.; Piomelli, D. Antidepressant-like activity and modulation of brain monoaminergic transmission by

- blockade of anandamide hydrolysis. Proc. Natl. Acad. Sci. U.S.A. 2005, 102, 18620–18625.
- (10) Kathuria, S.; Gaetani, S.; Fegley, D.; Valino, F.; Duranti, A.; Tontini, A.; Mor, M.; Tarzia, G.; La Rana, G.; Calignano, A.; Giustino, A.; Tattoli, M.; Palmery, M.; Cuomo, V.; Piomelli, D. Modulation of anxiety through blockade of anandamide hydrolysis. *Nat. Med.* **2003**, *9*, 76–81.
- (11) Piomelli, D. The molecular logic of endocannabinoid signalling. *Nat. Rev. Neurosci.* **2003**, *4*, 873–884.
- (12) Ahn, K.; Johnson, D. S.; Cravatt, B. F. Fatty acid amide hydrolase as a potential therapeutic target for the treatment of pain and CNS disorders. . *Expert Opin. Drug Discovery* **2009**, *4*, 763–784.
- (13) Minkkila, A.; Saario, S.; Nevalainen, T. Discovery and development of endocannabinoid-hydrolyzing enzyme inhibitors. *Curr. Top. Med. Chem.* **2010**, *10*, 828–858.
- (14) Seierstad, M.; Breitenbucher, J. G. Discovery and development of fatty acid amide hydrolase (FAAH) inhibitors. *J. Med. Chem.* **2008**, *51*, 7327–7343.
- (15) Otrubova, K.; Ezzili, C.; Boger, D. L. The discovery and development of inhibitors of fatty acid amide hydrolase (FAAH). *Bioorg. Med. Chem. Lett.* **2011**, *21*, 4674–4685.
- (16) Scott, C. W.; Tian, G.; Yu, X. H.; Paschetto, K. A.; Wilkins, D. E.; Meury, L.; Cao, C. Q.; Varnes, J.; Edwards, F. D. Biochemical characterization and in vitro activity of AZ513, a noncovalent, reversible, and noncompetitive inhibitor of fatty acid amide hydrolase. *Eur. J. Pharmacol.* **2011**, *667*, 74–79.
- (17) Eckelman, W. C.; Gibson, R. E.; Rzeszotarski, W. J.; Vieras, F.; Mazaitis, J. K.; Francis, B.; Reba, W. C. The Design of Receptor Binding Radiotracers. In *Principles of Radiopharmacology*; Colombetti, L., Ed.; CRC Press: New York, 1979; Vol. 1, pp 251–274.
- (18) Waterhouse, R. N. Determination of lipophilicity and its use as a predictor of blood-brain barrier penetration of molecular imaging agents. *Mol. Imaging Biol.* **2003**, *5*, 376–389.
- (19) Wyffels, L.; Muccioli, G. G.; Kapanda, C. N.; Labar, G.; De Bruyne, S.; De Vos, F.; Lambert, D. M. PET imaging of fatty acid amide hydrolase in the brain: synthesis and biological evaluation of an ¹¹C-labelled URB597 analogue. *Nucl. Med. Biol.* **2010**, *37*, 665–675.
- (20) Wilson, A. A.; Garcia, A.; Parkes, J.; Houle, S.; Tong, J.; Vasdev, N. [11C]CURB: Evaluation of a novel radiotracer for imaging fatty acid amide hydrolase by positron emission tomography. *Nucl. Med. Biol.* **2011**, 38, 247–253.
- (21) Wyffels, L.; Muccioli, G. G.; De Bruyne, S.; Moerman, L.; Sambre, J.; Lambert, D. M.; De Vos, F. Synthesis, in vitro and in vivo evaluation, and radiolabeling of aryl anandamide analogues as candidate radioligands for in vivo imaging of fatty acid amide hydrolase in the brain. *J. Med. Chem.* **2009**, *52*, 4613–4622.
- (22) Wyffels, L.; De Bruyne, S.; Blanckaert, P.; Lambert, D. M.; De Vos, F. Radiosynthesis, in vitro and in vivo evaluation of ¹²³I-labeled anandamide analogues for mapping brain FAAH. *Bioorg. Med. Chem.* **2009**, *17*, 49–56.
- (23) Skaddan, M. B.; Zhang, L.; Johnson, D. S.; Zhu, A.; Zasadny, K. R.; Coelho, R. V.; Kuszpit, K.; Currier, G.; Fan, K.-H.; Beck, E. M.; Chen, L.; Drozda, S. E.; Balan, G.; Niphakis, M.; Cravatt, B. F.; Ahn, K.; Bocan, T.; Villalobos, A. The synthesis and in vivo evaluation of [18F]PF-9811: a novel PET ligand for imagingbrain fatty acid amide hydrolase (FAAH). *Nucl. Med. Biol.* **2012**, *39*, 1058–1067.
- (24) Wilson, A. A.; Hicks, J. W.; Sadovski, O.; Parkes, J.; Tong, J.; Houle, S.; Fowler, C. J.; Vasdev, N. Radiosynthesis and evaluation of [11C-carbonyl]-labeled carbamatesas fatty acid amide hydrolase radiotracers for positron emission tomography. *J. Med. Chem.* **2013**, *56*, 201–209.
- (25) The medicinal chemistry efforts on the pyrazole series is the subject of another publication.
- (26) The potency drop was primarily due to the core change. There were two other changes from 3 to 4: chlorophenyl changed to chloropyridyl; primary amide changed to *N,N*-dimethyl tertiary amide. The former slightly decreased potency, and the latter slightly increased potency. They should cancel each other. Chloropyridyl was used here to further lower Log D.

- (27) Negishi, E.-I.; Hu, Q.; Huang, Z.; Wang, G.; Yin, N. Palladiumor Nickel-Catalyzed Cross-Coupling Reactions with Organozincs and Related Organometals. In *Chemistry of Organozinc Compounds*; Wiley: New York, 2006; Part 1, pp 457–553.
- (28) For its synthesis, see Supporting Information.
- (29) During the synthesis of the cold 6, the similar C-S coupling between methyl capped 23 and thiol 24 was high yielding (see Supporting Information).
- (30) The methylation of imidazole 8 to product 6 was highly regioselective where the regioisomer 7 was unable to detect from the crude product by NMR. In fact, compound 7 had to be prepared by a different route (see Supporting Information).
- (31) Dahlquist, F. W. The meaning of Scatchard and Hill plots. *Methods Enzymol.* **1978**, 48, 270–299.
- (32) Ueda, N.; Puffenbarger, R. A.; Yamamoto, S.; Deutsch, D. G. The fatty acid amide hydrolyse (FAAH). *Chem. Phys. Lipids* **2000**, *108*, 107–121